A Comparative Study of the p(2 × 2)-CO/M(111), M=Pt,Cu,Al Chemisorption Systems

Wingfield V. Glassey and Roald Hoffmann*

Department of Chemistry and Chemical Biology, Cornell University, Ithaca, New York 14853-1301

Received: October 25, 2000; In Final Form: February 17, 2001

We propose a model for CO chemisorption on late transition metal, noble metal, and main-group surfaces based on the results of energy partitioning studies of surface−CO bonding for the CO/M(111), M=Pt,Cu,Al chemisorption systems. Plane-wave density functional theory was used to calculate the chemisorption geometry for CO on the top, bridge, and hollow sites of the M(111) (M=Pt,Cu,Al) surfaces and to verify the experimentally determined preference for top site CO chemisorption on all three surfaces. To construct a chemically intuitive, molecular orbital based model of surface−CO bonding, an energy partitioning analysis of surface−CO bonding was carried out within a tight binding scheme based on the extended Hückel method. Although within this one-electron formalism we are no longer able to make quantitative assesments of bonding, we are able to readily extract surface−CO bonding trends. By expanding the orbital basis on CO to include energetically low-lying nonfrontier orbitals and explicitly evaluating the role of the surface s and p bands in surface−CO bonding, we note several discrepancies between our model and traditional, frontier orbital based models of surface−CO interaction. Especially important is the role of the CO(4σ) orbital. We note that for CO chemisorption on all three surfaces, the energetic preference for top site chemisorption is the result of a balance between the stabilization associated with the formation of the surface−CO bond and chemisorption-site-dependent changes in both C−O bonding and M−M (M=Pt,Cu,Al) bonding within the surface layer on chemisorbing CO. Further, by choosing to consider CO chemisorption on the Cu(111) surface as part of a continuous transition from CO chemisorption on late transition metal surfaces to CO chemisorption on sp-metal surfaces, we are able to assess the degree to which we may refer to copper as an sp-metal.

I. Introduction

The combination of an uncomplicated electronic structure and the ability to bind to a surface in both σ and π type modes has rendered carbon monoxide a prototypical absorbate for the study of surface−adsorbate interactions and the subject of numerous experimental and theoretical studies.

By choosing to study CO chemisorption on the Pt, Cu, and Al(111) surfaces, we anticipate being able to construct a detailed molecular orbital based picture describing surface−CO bonding for CO chemisorbed on late transition metal, noble metal, and main-group surfaces. We believe that the development of a conceptual model to treat surface−CO bonding over such a range of substrates represents a significant step toward a general understanding of surface−adsorbate interactions.

Our analysis of CO chemisorption is based on a hybrid computational approach. We begin by using density functional theory to obtain reliable chemisorption geometries and verify the energetic preference for top site CO chemisorption on all three surfaces. The changes in the electronic structure accompanying CO chemisorption are subsequently analyzed using a tight binding scheme developed within an extended Hückel framework. Hamilton population analysis—a partitioning of the total energy—serves as our principal "tool" for the analysis of surface−CO bonding. The energy partitioning scheme can be used to assess both the extent to which individual CO bands contribute to surface−CO bonding and the relative surface s, p, and d band contributions to the surface−CO chemisorption bond.[1]

* To whom correspondence should be addressed. E-mail: rh34@cornell.edu.

II. Computational Methodology, DFT Results, and Comparison with Experiment

In this study we have chosen to employ a hybrid computational approach to the study of CO chemisorption on the M(111) M=Pt,Cu,Al surfaces. We initially used the *fhi96md* code[2], which employs a finite temperature formulation of density functional theory and a plane-wave basis set, to generate two-dimensional slab models of the CO/M(111) M=Pt,Cu,Al chemisorption systems. The metal surface is modeled as a p(2 × 2) supercell based on the vectors **a** and **b** shown in Figure 1with three close-packed layers in the ...ABCABC... stacking pattern associated with a (111) termination of an fcc lattice.

The atoms were represented by soft norm-conserving pseudopotentials of the Troullier−Martins type[3] in the fully separable form of Kleinman and Bylander.[4] Plane-wave basis set expansions with energies up to 60 Ryd were used to represent the valence electron density of the CO/Pt(111) and CO/Al(111) chemisorption systems. A plane-wave expansion up to 80 Ryd was used to model CO chemisorption on the Cu(111) surface. Calculations with higher basis set energies suggest that these energies reproduce the total energy of the system to within 0.01 eV/atom. Prior to use, the pseudopotentials were tested for transferability and the absence of unphysical "ghost states" using Gonze's analysis.[5]

Before constructing slab models of the M(111), M=Pt,Cu,-Al surfaces, we first calculated the bulk fcc lattice constants for Pt,Cu, and Al using *fhi96md*. The bulk lattice constants were calculated using a 4 × 4 × 4 Monkhorst-Pack k-point set[6] within the Perdew−Zunger[7] parametrization of the local density approximation to exchange and correlation. The bulk lattice

10.1021/jp003922x CCC: $20.00
Published on Web 03/27/2001

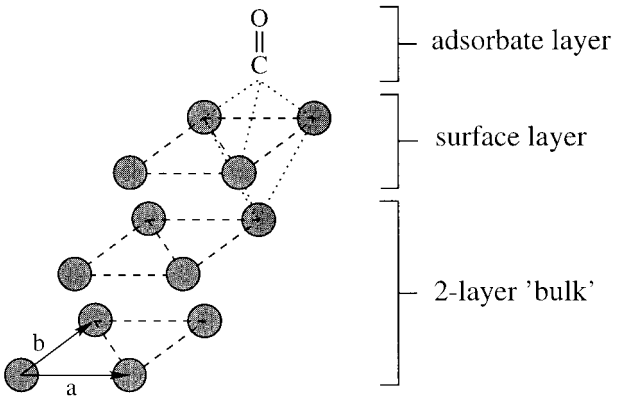

Figure 1. Schematic representation of the p(2 × 2) supercell (based on the vectors a and b) used to generate three layer slab models of the CO/M(111), M=Pt,Cu,Al chemisorption systems. The chemisorbed CO molecule is arbitrarily shown in the hcp hollow site.

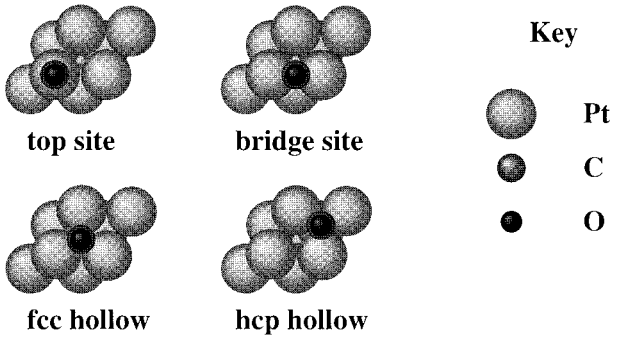

Figure 2. Top view of the p(2 × 2) supercell with CO chemisorbed in the top, bridge, fcc hollow, and hcp hollow sites. Only two layers of the three-layer slab are shown.

constants were calculated to be a(Pt) = 3.9078 Å, a(Cu) = 3.6414 Å, and a(Al) = 3.9966 Å, variations of 0.4%, 0.7%, and 1.3% with respect to previously reported literature values.[8]

Three-layer slab models of the M(111) M=Pt,Cu,Al surfaces were subsequently constructed using the calculated bulk lattice constants, and the top two layers of the slab relaxed using a damped Newtonian dynamics scheme[2] until the forces on the atoms were below 0.05 eV/Å. The validity of our surface models was verified by performing analogous relaxations on four-layer slab models representing the Pt(111), Cu(111), and Al(111) surfaces. In each case, the metal−metal bond lengths obtained from the relaxation differed by less than 0.03 Å from those obtained using a three-layer slab.

The atom positions within the three-layer slab models were subsequently fixed, and the equilibrium geometries for p(2 × 2) coverages of CO on the top, bridge, fcc hollow and hcp hollow chemisorption sites (see Figure 2) calculated. The CO layer was relaxed until the forces on the atoms were once more below 0.05 eV/Å. The calculated CO/M(111) M=Pt,Cu,Al chemisorption geometries are summarized in Table 1. Several computed CO chemisorption geometries for related chemisorption systems reported previously in the literature are also given in Table 1 for comparison.

From Table 1 we note that the chemisorption geometries obtained from our DFT computations are generally in good agreement with those reported in the literature. However, both the Al−C and C−O bond lengths for top site chemisorption on the Al(111) surface are significantly shorter than those reported in previous computational studies.[12] We note that the Al−CO bond lengths obtained for CO chemisorption in the bridge and hollow sites are significantly longer (∼2.0 Å and ∼2.1 Å, respectively) and are in agreement with the results of previous cluster-based calculations.[11,13] Thus, we are not overly concerned by the results of our geometry optimization for top site chemisorption on Al(111). Indeed, the relatively short Al−CO and C−O bond lengths computed for top site chemisorption are consistent with the picture of surface−CO bonding developed in subsequent sections of this paper.

TABLE 1: Summary of the Calculated Chemisorption Geometries for p(2 × 2) CO Coverages on the Pt, Cu, and Al(111) Surfaces

		bond length/Å[a]			
chemisorption system	bond	top	bridge	fcc hollow	hcp hollow
p(2 × 2)-CO/Pt(111)	Pt−C	1.86	1.94	2.14	2.07
	C−O	1.13	1.16	1.17	1.17
$(\sqrt{3} \times \sqrt{3})$R30−CO/Pt(111)[9]	Pt−C	1.86			
	C−O	1.14			
p(2 × 2)-CO/Cu(111)	Cu−C	1.82	1.89	2.00	2.01
	C−O	1.13	1.15	1.16	1.16
c(2 × 2)-CO/Cu(100)[10]	Cu−C	1.88			
	C−O	1.14			
p(2 × 2)-CO/Al(111)	Al−C	1.64	2.00	2.16	2.12
	C−O	1.11	1.18	1.18	1.19
CO/Al_{10} cluster[13]	Al−C	1.91			
	C−O	1.16		1.22	

[a] All bond lengths have an associated error of ± 0.02 Å. The C−O bond length for an isolated CO molecule was calculated to be 1.12 Å. CO chemisorption geometries reported previously in the literature for related chemisorption systems are also given for comparison.

In an analogous experiment, the top two layers of the three-layer Pt(111) slab model were allowed to relax along with p(2 × 2) coverages of CO chemisorbed in the top and bridge sites. In both cases, those platinum atoms in the surface layer directly bonded to chemisorbed CO moved between 0.03 and 0.04 Å further away from the underlying Pt atoms than in the unrelaxed slab. Those Pt atoms on the surface not directly bonded to chemisorbed CO moved between 0.02 and 0.03 Å closer to the underlying platinum atoms. These relatively minor perturbations of the atom positions in the surface layer do not significantly affect the results of our calculations. The magnitude of the approximation introduced by our choosing to fix the positions of the metal atoms when calculating the CO chemisorption geometry is quantified in a later section.

The surface and adsorbate relaxations were performed using a 2 × 2 × 1 Monkhorst-Pack k-point set within the Perdew−Zunger parametrization of the local density approximation to exchange and correlation. Comparative relaxations with 2 × 2 × 1, 4 × 4 × 1 and 6 × 6 × 1 k-point sets suggest that with a 2 × 2 × 1 set the atomic coordinates are accurate to within 0.01 Å. By deciding to use this geometrical measure of convergence, which is quite adequate for our purposes, we have not estimated the degree to which the total energy has converged with respect to the k-point mesh size. Despite this uncertainty, we compared the total energies for the p(2 × 2) coverages of CO on the various sites of the Pt(111), Cu(111), and Al(111) using the generalized gradient corrections of Perdew and Wang[14] and a 4 × 4 × 1 Monkhorst-Pack k-point set.

For all three surfaces, the top site was calculated to be the energetically preferred chemisorption site. Experimentally, at low coverages CO chemisorbs preferentially on the top site of both the Pt and Cu(111) surfaces. As the coverage increases, top-site chemisorption is accompanied by bridge site chemisorption.[15−18] For both surfaces a sharp $(\sqrt{3} \times \sqrt{3})R30°$ LEED pattern, corresponding to a one-third monolayer coverage of CO chemisorbed on the top-site, is observed. Thus, the preference for top site CO chemisorption at one-quarter monolayer coverage

TABLE 2: Extended Hückel Parameters Used in this Study

atom	orbital	H_{ii}/eV	ζ_1	ζ_2	c_1[a]	c_2[a]
Pt	5d	−13.3	6.013	2.696	0.6334	0.5513
	6s	−9.6	2.554			
	6p	−5.6	2.554			
Cu	3d	−14.9	5.950	2.300	0.5933	0.5744
	4s	−9.8	2.200			
	4p	−5.9	2.200			
Al	3s	−12.3	1.167			
	3p	−6.5	1.167			
C	2s	−21.4	1.625			
	2p	−11.4	1.625			
O	2s	−32.3	2.275			
	2p	−14.8	2.275			

[a] The coefficients c_1 and c_2 define the contributions of the individual Slater type orbitals in the double-ζ expansion used to represent the Pt 5d and the Cu 3d orbitals.

noted in our calculations is in accord with experimental observations.

Within the experimental community there is considerable debate as to whether CO chemisorbs molecularly or dissociatively on Al surfaces. There are reports of molecular chemisorption on both Al(111)[19] and Al(100)[20] single-crystal surfaces. It has been suggested that dissociative chemisorption on the Al(111) surface[21] is the result of CO interacting with oxide defects on the surface.

Computational studies based on cluster models of the Al(111) surface[11,13] also suggest that CO chemisorbs molecularly. However, the calculated preference is for chemisorption on the 3-fold hollow sites. The preference for higher coordinate chemisorption sites results from the use of nongradient corrected energy functionals; this is a well characterized failing of the local density approximation.[10,22] Thus we are satisfied that the results of our calculations mirror experimental findings, and we feel that the CO chemisorption geometry is sufficiently optimized to allow us to proceed with an analysis of surface−CO bonding.

III. Hamilton Population Analysis

To construct a detailed model of surface−CO bonding, we must be able to obtain information about the interaction between the chemisorbed CO layer and the surface bands. While our DFT calculations reliably reproduce the CO chemisorption geometries and the energetic preference for top site chemisorption on the Pt, Cu, and Al(111) surfaces, it is difficult to interpret the results of these calculations in the chemically familiar language of orbital interactions. Thus, for our analysis of surface−CO bonding, we choose to employ Hamilton population analysis, a partitioning of the total energy, within a tight binding formalism based on the extended Hückel method.[1] The extended Hückel calculations were performed with the YAeHMOP suite of programs.[23,24] A 4 × 4 × 1 Monkhorst-Pack k-point mesh was used to sample the irreducible wedge of the Brillouin zone. The extended Hückel parameters used are summarized in Table 2.

The Hamilton population formalism is, in essence, a partitioning of the total energy among the atoms and bonds. We define the partitioning by

$$E_{\mathrm{tot}} = \sum_{\substack{\mathrm{atoms}\\ i}} \mathrm{AHP}_i + \sum_{\substack{\mathrm{atoms}\\ i}} \sum_{\substack{\mathrm{atoms}\\ i>j}} \mathrm{BHP}_{ij} \qquad (1)$$

where the individual one-center (atomic or "on-site") Hamilton populations (AHPs) define the contributions to the total energy resulting from occupancy of the individual valence orbitals on each atom and the two-center (bond or "off-site") Hamilton populations (BHPs) define the energy contributions resulting from the interactions between the valence orbital basis on different atoms. A negative bond Hamilton population is interpreted as a *stabilizing* or *bonding* contribution to the total energy. Conversely a positive BHP is interpreted as an *antibonding* (repulsive) contribution to the total energy.

It is possible to reformulate eq 1 in a form that will allow us to define a surface−CO bond Hamilton population. We proceed by constructing a theoretical partitioning of the CO/M(111) chemisorption systems into three geometric fragments: the layer of chemisorbed CO molecules, the surface layer of the slab and the underlying "bulk" layers of the slab. The partitioning of the three-layer slab into surface and bulk "fragments" is prompted by our experiences with the application of Hamilton population analysis in the CO/Ni(100) chemisorption system.[1] In the CO/Ni(100) chemisorption system, the electronic structure changes accompanying chemisorption are localized in the surface layer of the Ni slab. Thus, by choosing to subdivide the slab into surface and bulk fragments, we anticipate focusing our attention on only those surface atoms that are intimately involved with bonding CO to the surface.

Within our surface−bulk−CO fragmentation scheme, eq 1 conveniently transforms as the sum over one- and two-center fragment Hamilton populations (FHPs) according to

$$E_{\mathrm{tot}} = \sum_{\substack{\mathrm{frags}\\ i}} \mathrm{FHP}_i + \sum_{\substack{\mathrm{frags}\\ i}} \sum_{\substack{\mathrm{frags}\\ j>i}} \mathrm{FHP}_{ij} \qquad (2)$$

In eq 2 we have partitioned the bond Hamilton population term from eq 1. Those BHPs involving atoms belonging to a particular fragment are combined with the AHPs for that fragment to give the (one-center) fragment Hamilton population for that particular fragment. The remaining bond Hamilton populations resulting from interactions between atoms belonging to two different fragments contribute to the two-center fragment Hamilton populations, FHP_{ij} (i,j = CO, surface, bulk). These two-center fragment Hamilton populations define the interactions between the surface, CO, and bulk fragments. Thus, by adopting the fragment-based partitioning of eq 2, we are able to unambiguously define the surface−CO "bond" Hamilton population to be the total interfragment Hamilton population, $\mathrm{FHP}_{\mathrm{surface-CO}}$. Once again "bond" Hamilton populations, such as those between entire fragments (the FHP_{ij}) are considered *bonding when negative* and *antibonding when positive*.

In subsequent discussions we will also focus a considerable amount of attention on two other fragment Hamilton populations resulting from the partitioning of eq 2. Formation of the surface−CO bond is accompanied by significant, chemisorption-site-dependent variations both in C−O bonding and in the bonding between the atoms belonging to the surface layer. Thus our attention is also focused on the two-center (BHP) components of the CO and surface layer fragment Hamilton populations, $\mathrm{FHP}_{\mathrm{CO}}$ and $\mathrm{FHP}_{\mathrm{surface}}$, respectively. We subsequently refer to these terms as the CO and surface bond Hamilton populations, respectively.

The final step toward a formalism capable of defining the contributions of the individual CO bands to the surface−CO bond Hamilton population is the transformation of our fragment-based analysis constructed using a valence orbital basis into a fragment-based analysis founded on the sets of molecular orbitals belonging to the individual geometric fragments. Such fragment molecular orbital descriptions of surface−CO bonding

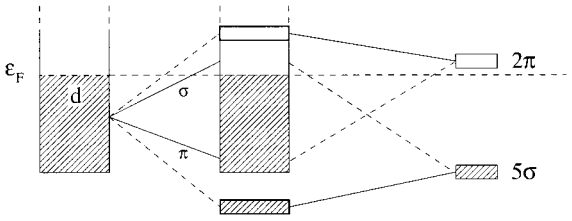

Figure 3. Schematic representation of Blyholder's model of surface−CO bonding. Solid and dashed lines are used, respectively, to indicate major and minor contributions to surface−CO bands.

appeal to our chemical intuition by allowing us to formulate our discussions in the language of frontier molecular orbital theory, and in doing so directly test the validity of traditional, frontier orbital based descriptions of surface−CO bonding.

IV. Constructing a Model for CO/M(111) (M=Pt,Cu,Al) Bonding

Traditionally the bonding between carbon monoxide and transition metal surfaces is described by Blyholder's model.[25] This model invokes simultaneous electron donation from the highest occupied MO of CO, the 5σ orbital, to the d bands on the metal surface and electron "back-donation" from the d bands of the metal surface to the lowest unoccupied MO on CO, the 2π orbital, as illustrated schematically in **1**.

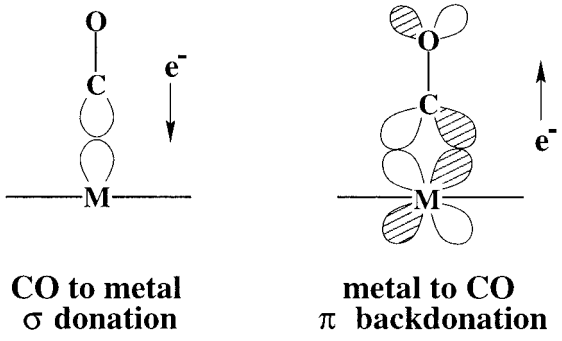

1

In the context of MO theory, Blyholder's model can be summarized by the schematic band interaction diagram shown in Figure 3. The interaction between the filled CO(5σ) band and the metal d band results in a band of formally M-CO bonding states in the vicinity of the bottom of the d band. These states are predominantly CO(5σ) in character. The corresponding M-CO antibonding bands are composed principally of contributions from the metal d band and are pushed toward the Fermi level (ϵ_F). For transition metals such as Ni and Pt, whose d band lies at a higher energy than the CO(5σ) band, some of the d states with σ symmetry are pushed above the Fermi level and the d(σ) occupancy drops. This is particularly evident when CO is chemisorbed on the top site, resulting in maximal overlap between the metal d(σ) states and the CO(5σ) band.

The π component of the M-CO interaction involves principally the interaction of the metal d band and the empty CO-(2π) band and results in M-CO bonding states which are predominantly metal d band in character distributed throughout the d band region. The corresponding antibonding states, which have mainly CO(2π) character, are found above the Fermi level.

In this contribution we will build on our earlier work on the CO/Ni(100) chemisorption system,[1] in which we proposed several extensions of the Blyholder model, and seek a qualitative model of CO chemisorption on both transition metal and sp-metal surfaces incorporating both additional CO bands and the s and p surface bands. Expansion of the "orbital basis" on CO to include nonfrontier orbitals (i.e., orbitals other than the 5σ and 2π) in order to describe surface−CO bonding is not a new idea. Indeed, previous studies by our group[26] and others[9,22,27,28] have indicated that in order to describe surface−CO bonding effectively it is necessary to consider both the bonding role of nonfrontier orbitals on CO and the surface s and p bands.

TABLE 3: Surface−CO Bond Hamilton Population Analysis for CO/Pt(111)[a]

	CO−Pt(111) HP/eV			
CO band	top	bridge	fcc hollow	hcp hollow
3σ	0.31	1.10	0.82	1.06
4σ	−4.56	−5.38	−4.93	−5.37
1π	0.41	0.43	0.28	0.31
5σ	−9.84	−9.90	−9.56	−9.73
2π	−4.67	−9.39	−8.91	−10.11
6σ	−0.10	−0.28	−0.24	−0.28
HP_{total}	−18.43	−23.46	−22.53	−24.12
$HP_\sigma \equiv HP(4\sigma+5\sigma)$	−14.40	−15.28	−14.49	−15.10
$HP(4\sigma+5\sigma+2\pi)$	−19.07	−24.67	−23.40	−25.21

[a] The contributions of the individual CO bands to the surface−CO bond Hamilton population are given for CO chemisorbed on the top, bridge, fcc hollow and hcp hollow chemisorption sites.

V. Is the Blyholder Model Valid for CO/Pt(111)?

To address the question of whether Blyholder's model provides a good description of surface−CO bonding, we calculated the contributions to the Pt−CO bond Hamilton population due to the individual CO bands for CO bound to the top, bridge, fcc hollow, and hcp hollow chemisorption sites on the Pt(111) surface (see Figure 2). The bond populations for the individual CO bands are summarized in Table 3.

Before proceding with our analysis of the Pt−CO bond population, it is worth noting that the total CO−Pt bond Hamilton populations given in Table 3 are *not* to be considered a measure of the relative stability of CO chemisorbed on the top, bridge, and hollow sites of the Pt(111) surface. Chemisorption involves not only the formation of a chemisorption bond between the CO molecule and the surface but also a site-dependent variation in the strength of both the C−O bond and the bonding between the atoms on the surface. We defer our discussion of the site-dependent variations in C−O and M−M (M=Pt,Cu,Al) bonding accompanying CO chemisorption until we have fully investigated the nature of the surface−CO chemisorption bond.

On examination of the bonding contributions due to the individual CO bands on each of the four chemisorption sites, we note that, for each site, in excess of 90% of the interaction is due to the 5σ, 2π, and 4σ CO bands. Back-bonding from the surface to the CO(2π) band is clearly a major contributor to surface−CO bonding. This is in accord with the Blyholder model, as is the unimportance of 1π interactions with the surface. There is also much more back-bonding in any bridging geometry, a point noted earlier.[26] Our focus here, however, is on the σ bonding, and in particular on the roles played by the CO 4σ and 5σ bands.

We note that for each chemisorption site, the CO(4σ) contribution to the surface−CO bond Hamilton population accounts for approximately one-third of the total σ component of the surface−CO bond. Similar observations were noted in our previous study of the CO/Ni(100) chemisorption system.[1] We conclude that in order to adequately describe the interactions between CO and late transition metal surfaces, such as the Pt-

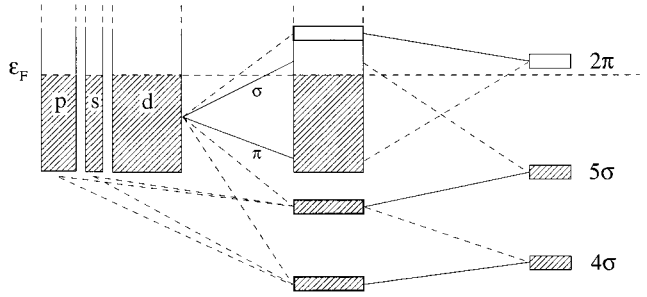

Figure 4. Schematic representation of orbital interactions in the CO/Pt(111) chemisorption system. Solid and dashed lines indicate respectively major and minor contributions to surface−CO bands.

(111) and Ni(100) surfaces, it is clearly necessary to expand Blyholder's model to include the CO(4σ) band.

Conceptually, inclusion of the CO(4σ) band does not alter Blyholder's model to any great extent. The CO(4σ) states are concentrated in a relatively narrow band below the CO(5σ) band, as shown schematically in Figure 4. Together with the CO(5σ) states, they constitute a "CO σ-donor function" analogous to the CO(5σ) band in Blyholder's model. The introduction of the CO(4σ) band results in a three-band model of surface−CO σ bonding that can best be understood in terms of a perturbation of the two-band model illustrated in Figure 3.

We begin our analysis by examining the topology of the CO 5σ (**2**) and 4σ (**4**) orbitals. Both orbitals are mixtures of the 2s and 2p orbitals on carbon and oxygen; the iconic representations **3** and **5** are a compromise between detail and simplicity. Clearly

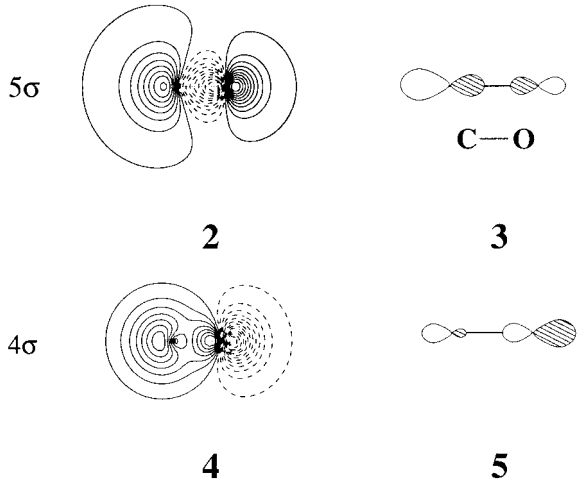

both the 5σ (**2**) and 4σ (**4**) orbitals have lone pair character at the carbon, directed away from the oxygen and toward the surface; the 5σ has somewhat more electron density reaching out toward the surface.

Mixing of the 4σ band into the higher lying 5σ and surface bands can be analyzed within the framework of perturbation theory. Second-order perturbation theory is required to describe the 4σ−5σ mixing. We proceed by first interacting the 4σ and 5σ bands of the $c(2 \times 2)$ array of chemisorbing CO molecules, which we denote 4σ^o and 5σ^o − separately with the surface as illustrated in **6**. We note that the ~5.3 Å separation between adjacent molecules in the $c(2 \times 2)$ array of chemisorbed CO molecules is sufficiently large to allow us to neglect through-space interactions between CO molecules. Thus we may consider the 4σ^o and 5σ^o bands to be composed of unperturbed 4σ and 5σ molecular orbitals on the individual CO molecules comprising the $c(2 \times 2)$ layer. The resulting 4σ' (**7**) and 5σ'

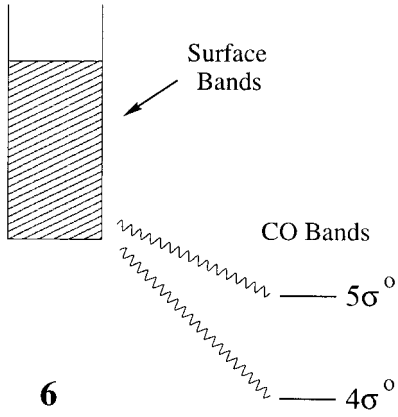

(**8**) states are not orthogonal and mix to give the final perturbed

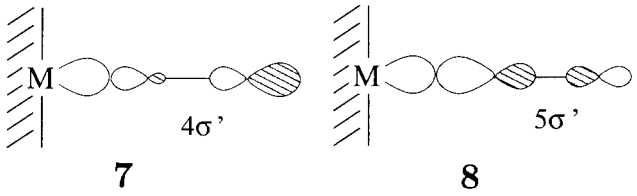

bands, which we refer to throughout this paper as the 4σ and 5σ bands. It is clear in this way how the 5σ band has in it not only 5σ^o character but also some 4σ^o character.

Another consequence of perturbation theory is that if two orbitals (bands) mix, the energetically lower orbital of the two mixes into itself the higher one in a bonding way. Conversely, the energetically higher orbital mixes into itself the lower level in an antibonding way. Thus, mixing of the 5σ' band into the 4σ' band to give the final "4σ" band results in increased surface−CO bonding within the 4σ band. As illustrated in **9**,

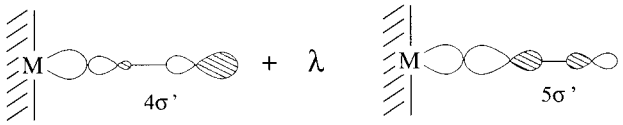

9

the 4σ band now contains surface−CO bonding contributions derived from both molecular 4σ^o and 5σ^o states (through the 4σ' and 5σ' states). The extent of mixing is characterized by the mixing coefficient, λ, a small positive number in the interval $0 < \lambda \ll 1$.

The increase in surface−CO σ bonding resulting from mixing the 5σ' band into the 4σ' band is accompanied by a reduction in surface−CO bonding that results from mixing of the 4σ' band into the energetically higher lying 5σ' band as illustrated schematically in **10**.

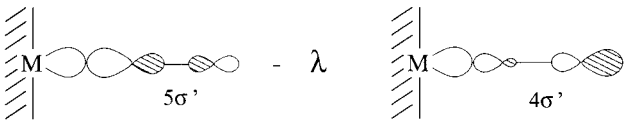

10

Thus, when evaluating the surface−CO(4σ^o) component of the surface−CO bond Hamilton population, we note a sizable bonding contribution (negative Hamilton population) arising from the 4σ band **9** and a somewhat smaller antibonding

TABLE 4: Decomposition of the surface−CO(4σ) Component of the Surface−CO Bond Hamilton Population for CO Chemisorbed on the Pt, Cu, and Al(111) Surfaces[a]

surface site	Pt−CO(4σ) HP /eV	4σ contribution	5σ contribution
top	−4.56	−9.91	5.35
bridge	−5.38	−11.96	6.58
fcc hollow	−4.93	−11.12	6.19
hcp hollow	−5.37	−11.89	6.52
surface site	Cu−CO(4σ) HP /eV	4σ contribution	5σ contribution
top	−3.32	−8.26	4.94
bridge	−4.41	−10.52	6.11
fcc hollow	−4.36	−10.47	6.11
hcp hollow	−4.35	−10.47	6.12
surface site	Al−CO(4σ) HP /eV	4σ contribution	5σ contribution
top	−2.04	−11.68	9.64
bridge	−2.75	−12.25	9.50
fcc hollow	−2.50	−12.22	9.72
hcp hollow	−3.26	−12.42	9.16

[a] The surface−CO(4σ) interaction is decomposed into contributions arising from within the energy windows containing the CO(4σ) and CO(5σ) DOS to indicate the extent to which the surface−CO(4σ) component of the surface−CO bond hamilton population is reduced by 4σ − 5σ mixing.

contribution to the surface−CO(4σ^o) bond Hamilton population resulting from the out-of-phase interaction between the surface and the 4σ^o component of the 5σ band **10**.

Throughout the remainder of this paper we will frequently refer to the surface−CO(4σ) and surface−CO(5σ) components of surface−CO bonding. When we do so we are really referring to the components of the surface−CO bond derived from the 4σ^o and 5σ^o bands.

In our previous study of the CO/Ni(100) chemisorption system,[1] we noted a significant reduction in the surface−CO(4σ) interaction resulting from mixing of the 4σ band into the energetically higher lying 5σ band **10**. We have also noted sizable reductions in the CO(4σ) contribution to surface−CO bonding for the Pt, Cu, and Al(111) surfaces. Table 4 summarizes the contributions to the surface−CO(4σ) bond Hamilton population arising from the 4σ and 5σ dominated bands in the CO/M(111), M=Pt,Cu,Al chemisorption systems. For both the Pt and Cu(111) surfaces, 4σ−5σ mixing reduces the potential for surface−CO(4σ) bonding by ∼50%. This effect is even more pronounced on the Al(111) surface, as evidenced by an ∼80% reduction in the surface−CO(4σ) bond Hamilton population in the region of the 5σ band.

In general, when attempting to develop models of surface−adsorbate interactions, we feel that it is important to assess the bonding potential of energetically low lying adsorbate orbitals, such as the CO 4σ orbital, with the potential to overlap significantly with the surface bands. Or, to put it another way, it is sometimes important not to reduce the set of hypothetical frontier orbitals (those orbitals we think are most involved in bonding) too much. Sometimes molecular orbitals that are not the HOMO or LUMO are important, as in the case of the CO(4σ) orbital.

It is interesting to note from Table 3 that the sum of the CO(4σ) and CO(5σ) contributions to the Pt−CO bond Hamilton population for CO chemisorbed on the top, bridge, and hollow sites of the Pt(111) surface is essentially constant. Thus, potentially, the CO chemisorption site preference on the Pt(111) surface is determined by the balance between the variation in the component of the Pt−CO bond Hamilton population derived from the CO(2π) band (back-bonding) and the site dependent variations in C−O bonding and Pt−Pt bonding within the surface.

TABLE 5: Surface s, p, and d Band Contributions to the CO−Pt(111) Bond Hamilton Population for CO Chemisorbed on the Top, Bridge, fcc Hollow, and hcp Hollow Chemisorption Sites of the Pt(111) Surface

surface site	Pt(s)-CO HP/eV	Pt(p)-CO HP/eV	Pt(d)-CO HP/eV
top	−7.00	−4.88	−7.47
bridge	−9.50	−4.98	−10.19
fcc hollow	−9.13	−4.96	−9.34
hcp hollow	−9.80	−5.02	−9.37

In Figure 4 we have also included the Pt(s) and Pt(p) bands in our model for Pt−CO interactions as a reflection of our finding that the Pt(s,p)-CO component of the Pt−CO interaction is greater than the Pt(d)-CO component for all four chemisorption sites considered. The s,p, and d band contributions to the Pt−CO(4σ, 5σ, 2π) interaction are detailed for all four chemisorption sites in Table 5. This clearly represents a further extension of Blyholder's model and was also noted in our previous study of the CO/Ni(100) chemisorption system.[1] Thus we conclude that for CO chemisorption on both the Pt(111) and Ni(100) surfaces, the surface−CO bonding can be described as metal sp-dominated bonding with the CO 4σ, 5σ, and 2π bands.

In the next section we begin our analysis of CO chemisorption on the Cu(111) surface in parallel with continued discussions of CO chemisorption on the Pt(111) surface. We will highlight the similarities and differences between the two chemisorption systems.

VI. CO Chemisorption on the Pt(111) and Cu(111) Surfaces

In general, CO chemisorption on noble metal surfaces such as the Cu(111) surface differs somewhat from CO chemisorption on late transition metal surfaces. For instance, the CO chemisorption energy on the various Cu surface sites is typically a factor of 2−3 smaller than for the corresponding site on the surfaces of late transition metals.[29] This trend also extends to alloyed transition metal surfaces whose principal surface component is Cu, for instance the (111) surface of the ordered transition metal alloy Cu_3Pt.[28] The situation is similar for CO chemisorption on other noble metal surfaces.[29,30]

Our discussion of CO chemisorption on the Pt(111) and Cu(111) surfaces is centered on bridge site chemisorption. From the Hamilton population analysis of Pt−CO bonding given in Table 3, we note that surface−CO bonding for CO chemisorbed on the bridge site is similar to that for CO chemisorbed in the fcc and hcp hollow sites. Top site CO chemisorption on Pt(111) differs somewhat and is characterized by a significantly lower CO(2π) contribution to the surface−CO bond Hamilton population. Thus we feel that an analysis of surface−CO bonding for bridge site chemisorption is more likely to be representative of the general features associated with CO chemisorption on the various sites of the Pt(111) and Cu(111) surfaces.

We begin our study of the CO/Cu(111) chemisorption system by examining how the band structure, in the form of the density of states (DOS), differs from the CO/Pt(111) chemisorption system. The total DOS for both systems is shown in Figure 5. The contributions of the 4σ, 1π, 5σ, and 2π bands of CO are also shown to illustrate how the bands of the CO layer interact with the surface bands.

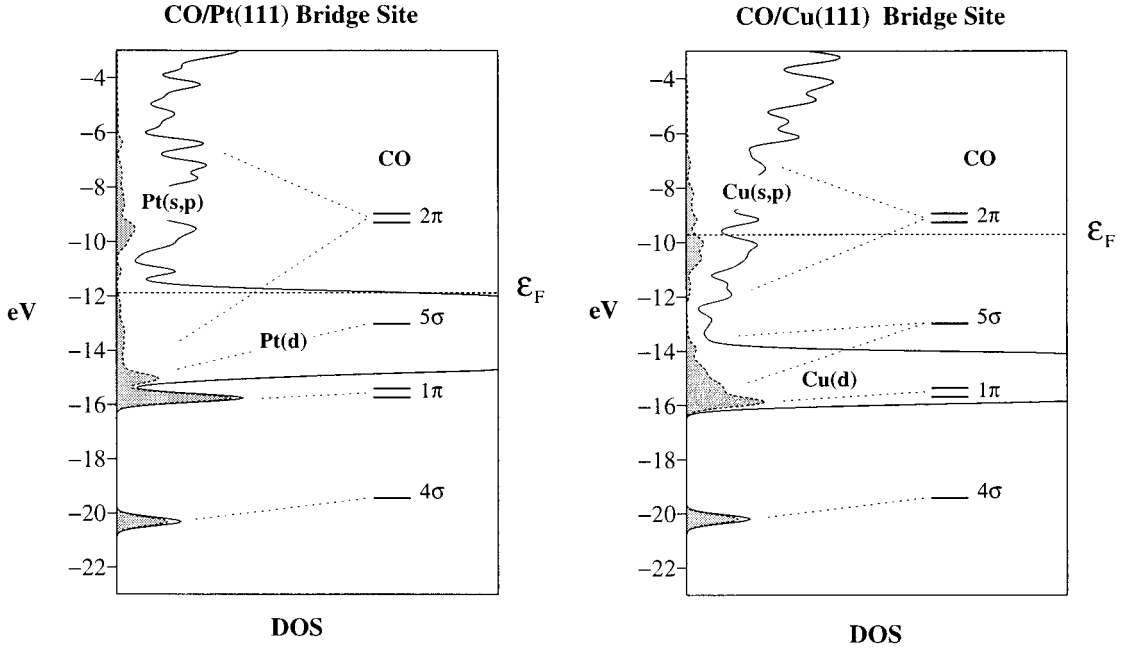

Figure 5. Density of states (DOS) for bridge site CO chemisorption on the Pt(111) and Cu(111) surfaces. The Fermi level (ϵ_F) is indicated by a horizontal dashed line. The Fermi level falls near the top of the narrow Pt(d) band and toward the bottom of the relatively broad Cu sp band. The molecular CO energy levels are superimposed on the DOS to indicate the orbital parentage of the DOS derived from the chemisorbed CO layer (shown shaded).

TABLE 6: Decomposition of the CO(5σ)−Cu(111) Hamilton Population in Terms of the σ, π, and δ Components of the Surface s, p, and d Bands[a]

	Cu(111) − CO(5σ) HP/eV					
Cu(111) site	s	p_σ	p_π	d_σ	d_π	d_δ
top	-4.33	−3.90	−0.07	−0.25	0.03	0.05
bridge	−4.99	−2.05	−1.93	0.01	−0.28	0.07
fcc hollow	−4.84	−1.79	−2.19	0.06	−0.28	0.05
hcp hollow	−4.85	−1.78	−2.19	0.06	−0.30	0.06

[a] The angular components of the surface bands are defined with respect to the surface normal.

TABLE 7: Decomposition of the CO(5σ)−Pt(111) Hamilton Population in Terms of the σ, π and δ Components of the Surface s, p, and d Bands

	Pt(111) − CO(5σ) HP/eV					
Pt(111) site	s	p_σ	p_π	d_σ	d_π	d_δ
top	−4.39	−2.82	−0.06	−2.74	−0.05	−0.04
bridge	−4.96	−1.23	−1.41	0.08	−1.81	−0.57
fcc hollow	−4.83	−1.19	−1.46	0.10	−1.64	−0.55
hcp hollow	−5.01	−1.06	−1.55	0.17	−1.68	−0.60

For both surfaces, the CO(4σ) band moves down a little and gives rise to a narrow band of states at approximately −20 eV. The CO(1π) band, which is essentially nonbonding with respect to the surface−CO interaction,[1] is identified as a sharp band in the DOS at approximately −16 eV. The CO(5σ) band for CO/Pt(111), a sharp peak at approximately −15 eV, is analogous to the 5σ band shown in Figures 3 and 4. In contrast, the CO-(5σ) band for CO/Cu(111), which now lies above the Cu(d) band, contributes to the total DOS throughout the d band region (approx. −14 to −16 eV). How are we to interpret this DOS on the basis of the rather general picture given in Figures 3 and 4?

One interpretation might be to assume that the CO(5σ) band interacts strongly with the Cu(d) band resulting in states with significant CO(5σ) character throughout the Cu(d) band. However, this interpretation can be ruled out quickly on calculating the bond Hamilton populations for the Cu(s), Cu-(p), and Cu(d) interactions with the CO(5σ) band. Examination of Table 6 illustrates, for all four chemisorption sites on the Cu(111) surface, the principally Cu(s,p) nature of the Cu−CO-(5σ) interaction. Indeed, the results summarized in Table 6 suggest that the Cu(d) band does not interact significantly with the CO(5σ) band.

We note that the Cu−CO(4σ) interaction is also dominated by the interactions involving the Cu s and p bands. Thus we propose that Cu−CO σ-bonding be described as CO to Cu(s,p) σ donation.

On the basis of an analysis of the surface−CO(5σ) bond Hamilton population for the CO/Pt(111) chemisorption system (Table 7) we conclude that the Pt−CO(5σ) interaction principally involves the Pt(s) and Pt(p) states—a feature that is by no means obvious from the DOS given in Figure 5. We also note from Table 7 that the Pt(d) states do make a significant, albeit minor, contribution to the Pt−CO(5σ) interaction. The same may be said for the interactions involving the CO(4σ) band. Thus, Pt−CO σ-bonding is also described as sp-dominated CO to metal σ-donation.

Finally, we consider the DOS arising from the CO(2π) band. In CO/Pt(111) the CO(2π) band mixes with the surface bands and results in a band of unoccupied states in the energy range approximately −11 to −6 eV, which are predominantly CO-(2π) in character. Within Blyholder's model (Figure 3) these bands correspond to formally antibonding interactions between the surface d bands and the CO(2π) band. The bonding counterparts of these states are found dispersed throughout the Pt d band, as indicated in Figure 5.

As for the case of Pt−CO(5σ) interactions, we must exercise caution and first analyze the results of a bond Hamilton population analysis of Pt−CO bonding before attempting to describe the Pt−CO(2π) interaction. The Pt s, p, and d band contributions to the Pt−CO(2π) interaction are summarized in

TABLE 8: Decomposition of the CO(2π)−Pt(111) Hamilton Population in Terms of the σ, π, and δ Components of the Surface s, p, and d Bands

	Pt(111) − CO(2π) HP/eV					
Pt(111) site	s	p_σ	p_π	d_σ	d_π	d_δ
top	−0.19	−0.05	−0.29	0.00	−4.07	−0.08
bridge	−1.34	−0.39	−0.39	−1.90	−3.90	−1.47
fcc hollow	−1.40	−0.40	−0.36	−1.47	−3.98	−1.33
hcp hollow	−1.56	−0.39	−0.44	−1.31	−4.72	−1.73

TABLE 9: Electron Occupancy of the CO(2π) Band as a Function of CO Chemisorption Site for CO Chemisorbed on the Pt, Cu, and Al(111) Surfaces

	CO(2π) occupation/e		
surface site	CO/Pt(111)	CO/Cu(111)	CO/Al(111)
top	0.32	1.12	3.83
bridge	0.64	1.90	3.62
fcc hollow	0.63	2.16	3.58
hcp hollow	0.70	2.16	3.55

TABLE 10: Decomposition of the CO(2π)−Cu(111) Hamilton Population in Terms of the σ, π, and δ Components of the Surface s, p, and d Bands

	Cu(111) − CO(2π) HP/eV					
Cu(111) site	s	p_σ	p_π	d_σ	d_π	d_δ
top	−1.43	−0.30	−2.28	−0.01	−0.89	0.02
bridge	−7.10	−3.34	−2.20	−0.10	−0.56	0.04
fcc hollow	−8.47	−3.76	−2.21	−0.09	−0.45	0.24
hcp hollow	−8.48	−3.82	−2.21	−0.10	−0.39	0.23

Table 8. For each of the chemisorption sites considered, we note that the Pt(d) contribution is, by far, the principal component of the interaction. This is again in agreement with our findings for the CO/Ni(100) chemisorption system,[1] and we conclude that Blyholder's M(d) → CO(2π) back-donation model is indeed a valid representation of surface−CO π-type interactions, at least for group 10 metal surfaces.

If we now consider Cu−CO(2π) interactions, we are faced with a quite different situation. For CO/Cu(111), the CO(2π) dominated bands, which were above the Fermi level for CO/Pt(111), are pushed partially below the Fermi level (Figure 5). Correspondingly, as indicated in Table 9, the occupancy of the CO(2π) band for CO chemisorption on the top, bridge, and hollow sites of the Cu(111) surface is significantly greater than for CO chemisorption on the corresponding sites of the Pt(111) surface.

We note that within our qualitative treatment of the electronic structure, the increased occupancy of the CO(2π) band for chemisorption on the Cu(111) surface is not, however, reflected in the DFT optimized C−O bond lengths summarized in Table 1. We suspect that our one-electron method overestimates the amount of electron back-donation from the surface to the CO(2π) band. Thus we make no attempt to quantify the increase in back-donation to the CO(2π) band on the Cu(111) surface, and we simply conclude that back-donation on the Cu(111) surface is greater than on the Pt(111) surface.

We note that for CO chemisorbed on the Cu(111) surface, the bandwidth for the CO(2π)-dominated bands is significantly smaller than for CO/Pt(111) and does not extend into the relatively low-lying Cu(d) band. Thus we might expect the Cu(d) contribution to Cu−CO(2π) interactions to be minor. This is indeed the case. Our analysis of the Cu s, p, and d band contributions to the Cu−CO(2π) bond Hamilton population is detailed in Table 10 and clearly indicates that the interaction is dominated by the Cu(s) and Cu(p) bands.

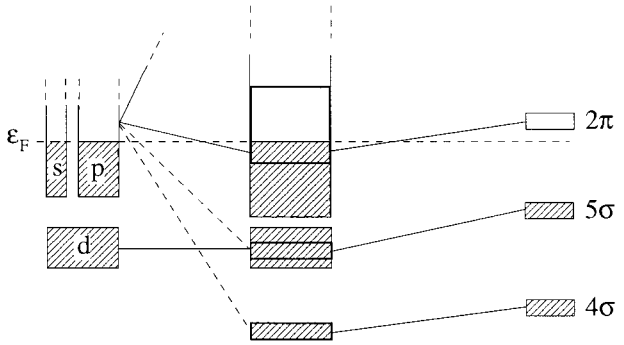

Figure 6. Schematic representation of orbital interactions in the CO/Cu(111) chemisorption system. Solid and dashed lines indicate, respectively, major and minor contributions to surface−CO bands.

Thus for copper, we must modify Blyholder's model of metal d-band dominated surface−CO π interaction in favor of an sp-dominated surface to CO(2π) back-donation model. Previous studies of CO chemisorption on Pt and Cu surfaces, by our group and others,[26,27] have also highlighted the potential for the surface s and p bands to contribute significantly to the π-component of the surface−CO bond.

Our conclusion is not surprising given that the copper d-orbitals are somewhat lower in energy and more contracted than those of platinum (Table 2). Both factors serve to reduce the potential for d_π − CO(2π) bonding (**11**). The significant

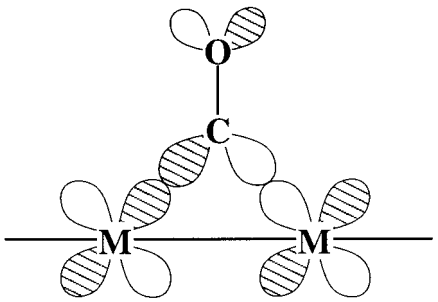

11

reduction in the surface d band contribution to surface−CO bonding on the Cu(111) surface prompts us to adopt a modified version of the surface−CO bonding schematic given earlier; this is given in Figure 6.

VII. CO Chemisorption on the Al(111) Surface

The Al(111) surface differs from both the Pt and Cu(111) surfaces in that the valence orbitals of the surface are constructed from a purely s and p orbital basis on each Al atom. The relatively low-lying Al(s) band opens up the possibility of increased surface−CO bonding resulting from the interaction of the Al(s) band with low-lying CO bands.

Another notable difference between the Al(111) surface and both the Pt and Cu(111) surfaces is the significantly greater filling of the s and p valence bands on the Al(111) surface. Formally the Pt, Cu, and Al(111) surfaces have, respectively 0, 1, and 3 sp electrons per surface atom. Thus we might expect to observe the consequences, if any, of increased s and p band filling when analyzing CO chemisorption on the Al(111) surface.

We begin our discussion of CO chemisorption on the Al(111) surface by examining whether the sp-dominated surface to CO(2π) back-donation model proposed for CO chemisorption

TABLE 11: Surface s, p_σ, and p_π Components of the CO(2π)−Al(111) Hamilton Population for CO Chemisorbed on the Top, Bridge, fcc Hollow, and hcp Hollow Surface Sites

	Al − CO(2π) bond HP/eV		
Al(111) site	s	p_σ	p_π
top	0.60	0.50	1.49
bridge	−0.07	−1.69	−1.35
fcc hollow	0.01	−2.44	−2.21
hcp hollow	0.10	−2.52	−2.69

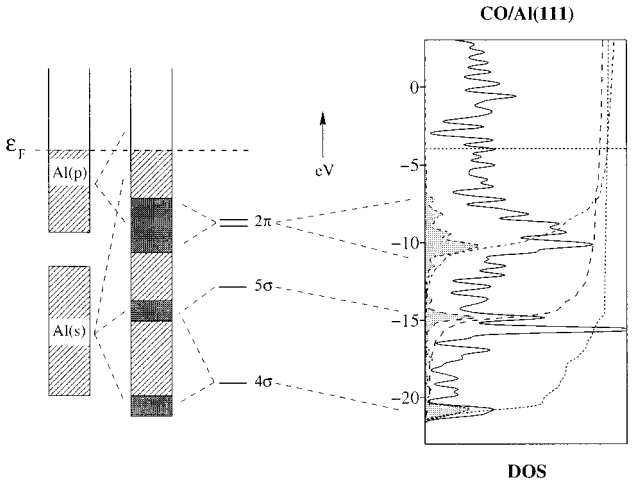

Figure 7. Schematic representation of bonding in the CO/Al(111) chemisorption system. The band interaction diagram on the left of the figure illustrates the interactions between the Al surface bands and the 4σ, 5σ, and 2π CO bands. Integration of the CO 4σ, 5σ, and 2π DOS, which is shown shaded against the total DOS for CO/Al(111) on the right of the figure, verifies that the CO bands are essentially localized in energy as shown in the schematic on the left of the figure. The CO 4σ, 5σ, and 2π integrations are illustrated by separate (dashed) lines.

on the Cu(111) surface can be applied to CO chemisorption on the Al(111) surface.

Table 11 details the contributions of the Al s, p_σ, and p_π bands to the Al−CO(2π) bond Hamilton population. From Table 11, it is clear that the CO(2π) band interacts principally with the Al(p) band. A significant drop in both the Al(p_σ) and Al(p_π) populations results as a portion of the Al(p) band is pushed above the Fermi level, as indicated in Figure 7. This p band dominated interaction is clearly distinct from the Cu(s) band dominated Cu(s,p)−CO(2π) interaction detailed in Table 10 and reflects the relatively large s band DOS in the region of the Fermi level for Cu(111).

As indicated in Table 9, the occupancy of the CO(2π) derived states is significant for CO/Cu(111) and even more so for CO/Al(111). The large CO(2π) occupancy for CO/Al(111) is primarily the result of an increase in the Fermi level with respect to CO/Cu(111), as evidenced by the position of the CO(2π) derived DOS for CO/Al(111) shown in Figure 7. From the plot of the CO(2π) component of the surface−CO bond Hamilton population given in Figure 8, we note that the bottom portion of the CO(2π) band is composed of surface−CO(2π) bonding states. The upper portion of the band is composed of the corresponding surface−CO(2π) antibonding states. Thus, filling the top half of the CO(2π) band results in a significant reduction in Al−CO(2π) bonding.

Similarly, the bottom of the 2π band for CO chemisorbed on the Cu(111) surface (Figure 5) is composed of surface−CO bonding states, and the upper portion of the band contains the corresponding surface−CO antibonding states. For bridge site chemisorption on the Cu(111) surface, the surface−CO(2π)

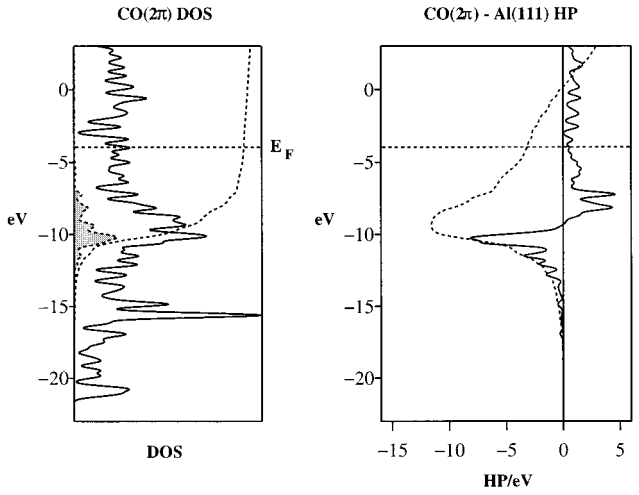

Figure 8. CO(2π) band components of the density of states (shaded) and surface−CO bond Hamilton population for CO chemisorbed on the Al(111) surface. The integrations of the 2π DOS and surface−CO(2π) Hamilton population are shown dashed.

bonding states are filled. Further increases in the occupancy of the CO(2π) band would result in filling of the surface−CO(2π) antibonding portion of the CO(2π) band and, consequently, decreased surface−CO(2π) bonding. Thus, save for the relatively large p band contribution to the surface−CO(2π) band interaction on the Al(111) surface, the interactions between the CO(2π) band and the Cu(111) and Al(111) surfaces are qualitatively similar.

If, on the basis of our analysis, we consider the CO(2π) band to be largely filled for CO chemisorbed on the Al(111) surface, it is perhaps surprising that CO does not dissociate on bonding to the surface. Despite our suspicions, experiments indicate that nondissociative chemisorption occurs on single-crystal Al(100) and Al(111) surfaces.[19,20] There are also several computational estimates of the CO chemisorption energy on both the Al(100) and Al(111) surfaces reported in the literature[11,13,28].

One particularly interesting result is the similarity between the CO chemisorption energies for CO chemisorbed on the Cu(111) and Al(111) surfaces calculated by Hammer et al.[28] using plane-wave density functional theory. The computed chemisorption energies on the Al(111) and Cu(111) surfaces (−0.49 eV and −0.62 eV, respectively[28]) serve to remind us that the sizable reduction in surface−CO bonding resulting from increased occupancy of the CO(2π) band for CO/Al(111) is only one of three potential contributors to the total energy change accompanying chemisorption. As pointed out earlier, in addition to the change in C−O bonding we must also take into account the changes in surface−CO bonding and M−M (M=Pt,Cu,Al) bonding within the surface layer when attempting to evaluate the chemisorption energy.

Tables 12 and 13 summarize, respectively, the contributions of the individual CO bands to the Cu−CO and Al−CO bond Hamilton populations and are analogous to the summary of Pt−CO bonding given in Table 3. We note from Tables 3, 12, and 13 that, for all four chemisorption sites considered, the CO(2π) contribution to the Al−CO bond Hamilton population is significantly smaller than the corresponding contribution on either the Pt(111) or Cu(111) surface. Indeed for CO chemisorbed on the top site of the Al(111) surface, the CO(2π) contribution to the surface−CO bond is actually repulsive. This is clearly the result of increased filling of the CO(2π) band for CO chemisorption on the Al(111) surface as indicated in Table 9. We note that surface−CO(2π) interactions are weakest for

TABLE 12: Surface−CO Bond Hamilton Population Analysis for CO/Cu(111)[a]

	CO−Cu(111) HP/eV			
CO band	top	bridge	fcc hollow	hcp hollow
3σ	0.09	0.53	0.55	0.55
4σ	−3.32	−4.40	−4.35	−4.35
1π	0.28	0.55	0.51	0.51
5σ	−8.47	−9.18	−8.99	−9.02
2π	−4.90	−13.23	−14.76	−14.78
6σ	−0.06	−0.18	−0.19	−0.19
HP_{total}	−16.38	−25.92	−27.21	−27.28
$HP_\sigma \equiv HP(4\sigma+5\sigma)$	−11.79	−13.58	−13.34	−13.37
$HP(4\sigma+5\sigma+2\pi)$	−16.69	−26.81	−28.00	−28.15

[a] The contributions of the individual CO bands to the surface−CO bond Hamilton population are given for CO chemisorbed on the top, bridge, fcc hollow, and hcp hollow chemisorption sites.

TABLE 13: Surface−CO Bond Hamilton Population Analysis for CO/Al(111)[a]

	CO−Al(111) HP/eV			
CO Band	top	bridge	fcc hollow	hcp hollow
3σ	2.34	2.59	2.61	2.57
4σ	−2.04	−2.75	−2.50	−3.26
1π	1.86	1.09	0.80	0.79
5σ	−6.75	−7.63	−7.56	−8.02
2π	2.59	−3.11	−4.64	−5.11
6σ	−0.20	−0.19	−0.19	−0.15
HP_{total}	−2.20	−10.00	−11.48	−13.18
$HP_\sigma \equiv HP(4\sigma+5\sigma)$	−8.79	−10.38	−10.06	−11.28
$HP(4\sigma+5\sigma+2\pi)$	−6.20	−13.49	−14.70	−16.39

[a] The contributions of the individual CO bands to the surface−CO bond Hamilton population are given for CO chemisorbed on the top, bridge, fcc hollow, and hcp hollow chemisorption sites.

TABLE 14: C−O Bond Hamilton Population for CO Chemisorbed on the Top, Bridge, fcc Hollow and hcp Hollow Sites of the Pt, Cu, and Al(111) Surfaces

	C−O bond HP/eV		
surface site	CO/Pt(111)	CO/Cu(111)	CO/Al(111)
top	−40.62	−35.01	−16.52
bridge	−37.36	−29.68	−18.99
fcc hollow	−36.69	−27.82	−19.26
hcp hollow	−36.09	−27.88	−19.51

top site chemisorption, for which interactions between the CO-(2π) orbitals and the surface p(σ) orbitals of the surface atom directly below the CO molecule are symmetry forbidden. Thus for CO chemisorption on the bridge and hollow sites, more of the Al(111) surface states are pushed above the Fermi level. This results in a reduction in the occupancy of the CO(2π) band (see Table 9) and a net stabilizing surface−CO(2π) interaction. Correspondingly, in Table 14 we note an increase in the C−O bond Hamilton population for CO chemisorbed on the bridge and hollow sites of the Al(111) surface.

An analogous reduction in the surface−CO(2π) interaction for CO chemisorbed on the top site of the Cu(111) surface results in less CO(2π) derived DOS below the Fermi level (see Figure 5) and a reduction in the occupancy of the CO(2π) bands (see Table 9). Thus, in contrast to chemisorption on the Al-(111) surface, the magnitude of the C−O bond Hamilton population for top site chemisorption on the Cu(111) surface is greater than for CO chemisorption on the 2- and 3-fold sites of the Cu(111) surface as indicated in Table 14.

We note that the occupancy of the CO(2π) band for top site chemisorption on the Al(111) surface could, potentially, have been greater still. On increasing the Al−CO bond length for top site chemisorption from the DFT optimized value of 1.64 Å (Table 1) to 1.90 Å (the value obtained in previous cluster-based studies of Al−CO bonding[13]), the interaction between the CO(2π) band and the surface bands decreases. As a result, more of the CO(2π) band is found below the Fermi level and the occupancy of the CO(2π) band increases. In other words, as CO is moved further from the surface, an increased amount of charge is transferred from the surface to the CO(2π) orbitals. The increased occupancy of the CO(2π) orbitals results in reduced C−O bonding and a corresponding increase in the total energy of the chemisorption system. This is, we believe, the reason for the significantly shorter metal-to-carbon bond length calculated for top site CO chemisorption on the Al(111) surface.

We note that for the case of CO chemisorption on the Al(111) surface, all but one of the CO bands, the very high lying 6σ band, play significant roles in the surface−CO interaction. This prompts us to further extend the CO$(4\sigma, 5\sigma, 2\pi)$ orbital basis used to describe surface−CO bonding for both the Pt(111) and Cu(111) surfaces to include both the 3σ and 1π CO bands. Both of these bands interact principally with the Al(p_σ) bands directed along the surface normal, giving rise to repulsive interactions for each of the four chemisorption sites considered. These interactions involve filled bands and are analogous to the classic two-orbital-four-electron repulsion shown in scheme 12.

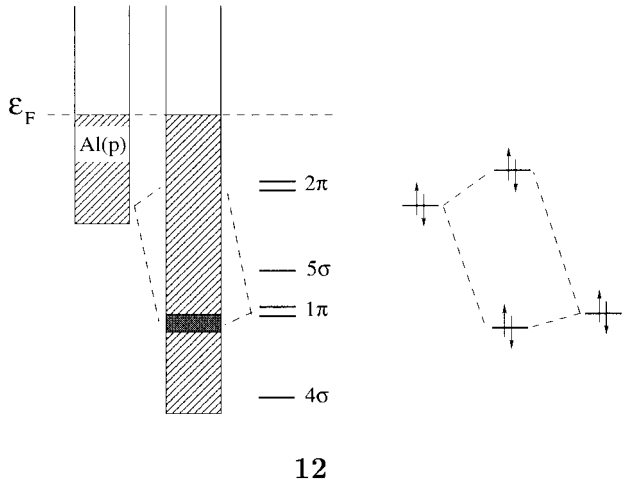

12

We note that the sum of the Al−CO(4σ), Al−CO(5σ), and Al−CO(2π) interactions given in Table 13 successfully reproduces the site-dependent variation in the surface−CO bond Hamilton population (HP_{total}). Thus, if we seek to model the variation in surface−CO bonding with respect to the chemisorption site, we can revert to the 4σ, 5σ, 2π orbital basis on CO used to describe surface−CO bonding for the Pt(111), Cu-(111), and Ni(100)[1] surfaces. Further, we note that for CO chemisorbed on the Cu and Al(111) surfaces, both the σ and π components of the surface−CO bond Hamilton population, detailed in Tables 12 and 13 respectively, exhibit a significant site dependence. This is in contrast to our earlier observation that the σ component of the Pt−CO bond Hamilton population (Table 3) is essentially site independent. Thus, in general, we must consider site-dependent variations in the surface−CO bond Hamilton population to be the result of changes in both the σ and π components of the interaction.

VIII. A Closer Look at Surface−CO(4σ,5σ) Bonding on the Pt(111), Cu(111) and Al(111) Surfaces

We begin our analysis by noting significant contributions to the CO/Al(111) DOS in Figure 7 in the energy window between

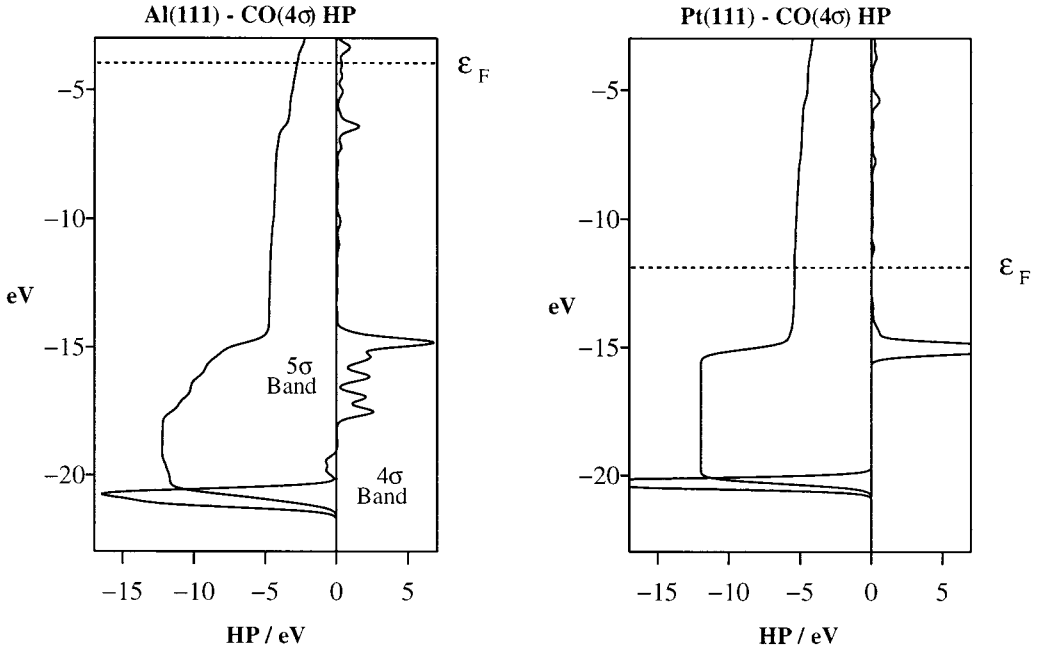

Figure 9. Plots of the CO(4σ) − M(111), M=Al,Pt components of the surface−CO bond Hamilton population for CO chemisorption on the bridge site. For both surfaces the significant contributions to the surface−CO(4σ) Hamilton population arising from the CO(4σ) dominated DOS peak at approximately −21 eV for CO/Al(111) and approximately −20 eV for CO/Pt(111) is tempered by mixing of the CO 4σ and 5σ bands throughout the energy window containing the CO(5σ) derived DOS.

the predominantly 4σ band at approximately −21 eV and the 5σ band at approximately − 15 eV. These 4σ contributions to the DOS, which sum to approximately 30% of the total 4σ DOS (as shown by the 4σ DOS integration curve in Figure 7), arise from strong Al(s)−CO(4σ) interactions. This is in marked contrast to the situation for both the Pt and Cu(111) surfaces whose s band DOS lies significantly higher in energy than that of the Al(111) surface. For both of these surfaces, the surface(s)−CO(4σ) interactions are weaker than those for CO chemisorbed on the Al(111) surface, and CO(4σ) contributions to the DOS are confined to relatively narrow low-lying bands of states as illustrated in Figure 5.

Thus, for CO chemisorption on the Pt and Cu(111) surfaces, we regard interactions between the surface s band and the CO(4σ) band as a perturbation on the surface s band interaction with the CO(5σ) band. This is clearly not the case for CO chemisorption on the Al(111) surface. The much improved "energy match" between the surface s band and the CO(4σ) band for the CO/Al(111) chemisorption system prompts us to consider the interaction between the surface s band and both the CO(4σ) and CO(5σ) bands as significant.

Sizable interaction between the Al(s) band and both the CO(4σ) and CO(5σ) bands potentially results in surface−CO bands that exhibit both significant 4σ and 5σ character. From the integration of the CO(4σ) DOS in Figure 7, we note that the bands in the vicinity of the CO(5σ) dominated band at approximately −15 eV in Figure 7 have significant 4σ character. Indeed, from the integration of the CO(5σ) DOS in Figure 7, we note that the contribution to the CO(5σ)-derived DOS from these states is less than the CO(4σ) contribution. Thus we choose to describe these states as formally surface−CO(4σ) antibonding states with some CO(5σ) character.

Clearly the Al(111) surface interacts to a greater extent with the low-lying CO σ bands than do either the Pt or Cu(111) surfaces. We now consider the implications of the increase in surface−CO(4σ) interaction with respect to the extent of the rehybridization between the CO 4σ and 5σ bands for CO chemisorbed on the Al(111) surface.

The sizable reduction in the Al−CO(4σ) contribution to the Al−CO bond Hamilton population that occurs throughout the energy window containing CO(5σ) contributions to the DOS in Figure 9 (approx. −18 eV through −14 eV) is completely analogous to that shown on the right-hand side of Figure 9 for CO chemisorbed on the Pt(111) surface. The Pt−CO(4σ) and Al−CO(4σ) bond Hamilton populations illustrated in Figure 9 are summarized in Table 4.

The introduction of surface−CO(4σ) antibonding states immediately below the CO(5σ) dominated band at approximately −15 eV results in an increase in the amount of 4σ−5σ mixing on binding CO to the Al(111) surface relative to that for CO chemisorbed on the Pt and Cu(111) surfaces and a correspondingly lower CO(4σ) contribution to surface−CO bonding.

IX. Frozen Band Models of CO Chemisorption

In this section we examine the extent to which we may use frozen band models, based on the electronic structure of the CO/Pt(111) and CO/Al(111) chemisorption systems, to describe CO chemisorption on the Pt, Cu, and Al(111) surfaces.

The CO/Pt(111), CO/Cu(111), and CO/Al(111) chemisorption systems are representative of CO chemisorption systems with, respectively, 0, 1, and 3 sp electrons per surface atom. We begin our frozen band study by analyzing the changes in the contributions made by the individual CO molecular orbitals to the surface−CO bond Hamilton population on simply adding additional electrons to the CO/Pt(111) chemisorption system. Within our extended Hückel treatment of the electronic structure, the bands of the CO/Pt(111) chemisorption system remain unchanged on adding electrons to the system. Thus we are afforded the opportunity to assess the extent to which the additional electrons that occupy the s and p bands on the Pt-(111) surface (see Figure 5) determine the magnitude of the individual CO molecular orbital contributions to surface−CO bonding on the Cu(111) and Al(111) surfaces. Table 15 summarizes the surface−CO bonding contributions due to the

TABLE 15: the Individual CO Band Contributions to surface−CO Bonding Calculated Using the Frozen Band Approximation with 0,1, and 3 *sp*-electrons Per Surface Atom[a]

	contribution to surface−CO bonding/eV		
CO band	$d^{10}(sp)^0$ [Pt]	$d^{10}(sp)^1$ ["Cu"]	$d^{10}(sp)^3$ ["Al"]
3σ	1.10	1.12	1.20
4σ	−5.38	−5.16	−4.27
1π	0.43	0.74	1.45
5σ	−9.90	−9.26	−8.15
2π	−9.39	−14.30	−4.33
6σ	−0.28	−0.31	−0.39
HP_{total}	−23.42	−27.17	−14.49

[a] The Frozen Band Model Is Based on the Electronic Structure of the CO/Pt(111) chemisorption system.

TABLE 16: Individual CO Band Contributions to Surface−CO Bonding Calculated Using the Frozen Band Approximation with 0, 1, and 3 sp electrons Per Surface Atom[a]

	Contribution to surface−CO Bonding/eV		
CO band	$(sp)^0$ ["Pt"]	$(sp)^1$ ["Cu"]	$(sp)^3$ [Al]
3σ	1.09	1.97	2.59
4σ	−9.28	−4.57	−2.75
1π	−1.89	−0.62	1.09
5σ	−2.55	−9.72	−7.63
2π	−0.31	−3.77	−3.11
6σ	−0.06	−0.09	−0.19
HP_{total}	−13.00	−16.80	−10.00

[a] The frozen band model is based on the electronic structure of the CO/Al(111) chemisorption system.

individual CO molecular orbitals for the CO/Pt(111) chemisorption system with 0, 1, and 3 sp electrons per surface atom.

From Table 15 we note that the CO(5σ) contribution to surface−CO bonding decreases on adding additional electrons to the CO/Pt(111) chemisorption system. This reflects the trend in the 5σ contribution to surface−CO bonding for CO chemisorbed on the various sites of the Pt(111) (Table 3), Cu(111) (Table 12), and Al(111) (Table 13) surfaces. Similarly, the reduction in the 4σ contribution to surface−CO bonding on increasing the sp electron count on the surface reflects the trend in surface−CO(4σ) bonding noted for the CO/Pt(111), CO/Cu(111), and CO/Al(111) chemisorption systems. From Table 15, we also note that the frozen band model based on the CO/Pt(111) chemisorption system successfully reproduces the trend in the CO(2π) contribution to surface−CO bonding on the Pt, Cu, and Al(111) surfaces. On noting that the 4σ, 5σ, and 2π contributions to surface−CO bonding obtained using the frozen band approximation are, generally, in good agreement with those for the CO/Cu(111) and CO/Al(111) chemisorption systems (Tables 12 and 13 respectively), we are tempted to conclude that the filling of the surface s and p bands is the principal factor determining the nature of the surface−CO chemisorption bond.

However, if we now focus our attention on the corresponding frozen band model based on the electronic structure of the CO/Al(111) chemisorption system (Table 16) we note that the relative 4σ, 5σ, and 2π band contributions to surface−CO bonding for 0, 1, and 3 sp electrons per surface atom do not always follow those calculated for CO chemisorption on the Pt(111), Cu(111), and Al(111) surfaces (Tables 3, 12, and 13, respectively). Most noteworthy is the failure of the Al(111)-based model to reproduce the monotonic decrease in surface−CO(5σ) bonding for CO chemisorbed on the various sites of the Pt(111), Cu(111), and Al(111) surfaces. Within the Al(111)-based model, the CO(5σ) contribution to Pt−CO bonding is significantly lower than expected.

The Al(111)-based model does somewhat better when predicting the relative magnitudes of the surface−CO(2π) components of Pt−CO, Cu−CO, and Al−CO bonding. However, we note that the reduction in surface−CO(2π) bonding noted previously for chemisorption on the Al(111) surface is not reproduced by the Al(111)-based model. Indeed the CO(2π) contribution to surface−CO bonding is predicted to be an order of magnitude greater on the Al(111) surface than on the Pt(111) surface. The Al(111)-based model does, however, succeed in reproducing the monotonic decrease in {Pt,Cu,Al}-CO(4σ) bonding given in Tables 3, 12, and 13.

Clearly, the Pt(111)- and Al(111)-based frozen band models differ somewhat in their description of surface−CO bonding as a function of the s and p band electron count. Given the significant differences between the nature of the surface orbitals for the Pt(111) and Al(111) surfaces, in particular the presence of the Pt(d) band, we conclude that a frozen band model of surface−CO bonding cannot fully account for the significant differences in surface−CO bonding resulting from differences in the surface electronic structure.

Work is currently underway to investigate the applicability of frozen band models of CO chemisorption on a variety of pure and alloyed transition metal surfaces composed of both early and late transition metals.[31]

X. CO Chemisorption on the M(111) M=Pt,Cu,Al Surfaces

We now summarize the results of our analyses of surface−CO bonding in the CO/M(111) M=Pt,Cu,Al chemisorption systems and highlight the changes in surface−CO bonding that accompany the transition from CO chemisorption on late transition metal surfaces such as the Pt(111) surface, to CO chemisorption on sp metal surfaces such as Al(111).

We begin by considering surface−CO σ-bonding on the Pt(111) surface. On the basis of our bond Hamilton population study of CO/Pt(111) bonding, we earlier concluded that the σ-component of the Pt−CO bond was dominated by interactions involving the s and p surface states. We previously reported similar findings for the CO/Ni(100) chemisorption system.[1] Our results prompt us to modify Blyholder's CO → M(d) σ-donation model (Figure 3) in favor of a CO → M(s,p,d) σ-donation model (Figure 4) dominated by interactions between the CO bands and the surface s and p bands.

For CO chemisorption on the Cu(111) and Al(111) surfaces, which we choose to consider as representative examples of CO chemisorption on noble and sp metal surfaces respectively, our metal sp band dominated CO → M(s,p,d) σ-donation model for late transition metal surfaces transforms smoothly into a CO → M(s,p) σ-donation model. In this respect we note that copper behaves as an sp metal.

For each surface studied, we note a significant reduction in the potential for surface−CO(4σ) bonding as the result of a rehybridization of the 4σ and 5σ CO bands on bonding CO to the surface. Despite this reduction in surface−CO(4σ) interaction, we still note significant surface−CO(4σ) bonding, principally involving the surface s and p bands. Thus we wish to further modify Blyholder's model by explicitly including the CO(4σ) orbital in our "bonding basis" on CO as illustrated schematically in Figure 4.

Indeed, for sp metal surfaces such as Al(111), whose s band is found at significantly lower energies than the s band of either transition or noble metal surfaces, one should even include the

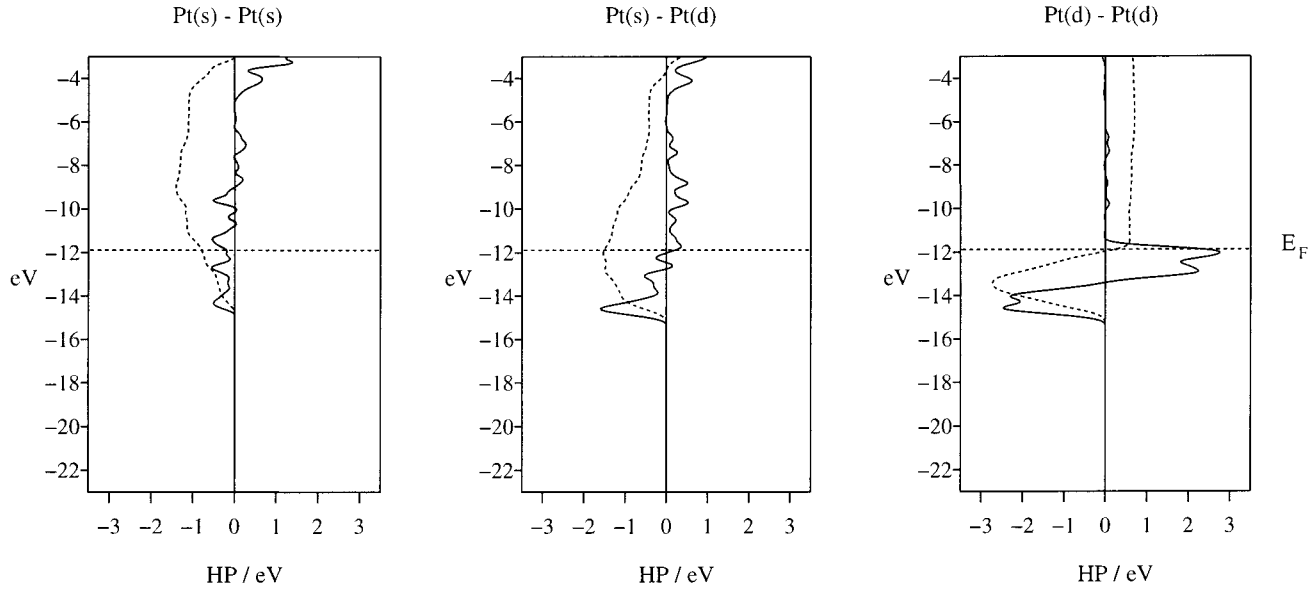

Figure 10. Energy resolved s−s, s−d, and d−d components of a Pt−Pt surface bond belonging to a clean Pt(111) surface. The numerical value of each component is given by the intersection of the integration (vertical dashed line) and the Fermi level, ϵ_F.

energetically low lying CO(3σ) band in a quantitative analysis of surface−CO σ bonding.

In contrast to the relative (and understandable) shortcomings of Blyholder's model when attempting to describe the σ component of surface−CO interactions, we find that Blyholder's model represents a fair description of surface−CO π interactions for both the CO/Pt(111) and CO/Ni(100) chemisorption systems. In both cases, a bond Hamilton population analysis attributes ~90% of the π interaction to the surface d band. Thus for CO chemisorbed on surfaces composed of late transition metals such as Pt and Ni, Blyholder's surface d band → CO(2π) back-donation model of π interactions is a good description.

We note that the CO(2π) contributions to surface−CO bonding on both the Cu(111) and Al(111) surfaces have a somewhat different origin from those for CO chemisorption on late transition metal surfaces. For CO chemisorbed on the Cu(111) surface, the CO(2π) band interacts strongly with both the surface s and p bands. This results in a portion of the CO(2π) band lying below the Fermi level. The Al(p) band dominates the π component of surface−CO bonding for CO chemisorbed on the Al(111) surface. A significantly higher Fermi level results in an essentially filled CO(2π) band and a sizable reduction in surface−CO(2π) bonding compared with that for CO chemisorbed on the Pt and Cu(111) surfaces.

Clearly, to describe the π component of surface−CO bonding in the CO/Cu(111) and CO/Al(111) chemisorption systems we must extend Blyholder's concept of surface(d) → CO(2π) back-donation to include the surface s and p bands. We propose a transition from surface d band dominated surface−CO π back-donation for CO chemisorption on late transition metal surfaces, such as the Pt(111) surface, to surface p band dominated back-donation on main-group surfaces such as the Al(111) surface. The π component of the CO−Cu(111) chemisorption bond, which includes significant contributions from both the Cu s and p bands, represents a "midpoint" in the transition. This is a reflection of both the reduction in surface d band contributions to the chemisorption bond resulting from a more contracted, energetically low lying, surface d band, and a high lying s band. Thus in this context, the Cu(111) surface, which we consider to be representative of noble metal surfaces in general, behaves neither as a transition metal surface nor a main-group surface.

Thusfar in our discussions we have focused on describing the surface−CO chemisorption bond. To appreciate fully the "mechanics" of the chemisorption process we must also examine the changes in surface and adsorbate bonding that accompany the chemisorption process.

XI. Changes in Surface and Adsorbate Bonding on CO Chemisorption

The chemisorption process involves not only the formation of the surface−adsorbate bond but it also results in significant changes in the bonding both on the surface and within the chemisorbing molecule. As we will see, the changes in both the electronic structure of the surface and the adsorbate accompanying CO chemisorption are strongly dependent on the CO chemisorption site.

We begin by considering the interaction between CO and the Pt(111) surface. The relatively minor role of the Pt(d) band in the σ component of the Pt−CO interaction is the direct result of greater orbital overlap between the CO σ bands and the surface s and p bands. This sizable interaction with the surface s and p bands significantly reduces the number of s and p states available for Pt−Pt bonding in the vicinity of chemisorbed CO. To illustrate this point, consider the s−s, s−d, and d−d components of the Pt−Pt bond Hamilton population for a Pt−Pt bond belonging to the surface layer of a 3-layer Pt(111) slab model given in Figure 10.

The d−d component of the Pt−Pt bond Hamilton population in Figure 10 highlights the bonding nature of the Pt(d)−Pt(d) interaction toward the bottom of the d band at approximately −14 eV, a negative (stabilizing) contribution to the Pt−Pt bond Hamilton population, and the antibonding nature of the Pt(d)−Pt(d) interaction toward the top of the d band at approximately −12 eV. The energetically higher lying Pt(s) band (see Figure 5) mixes into the Pt(d) band in a bonding way, as illustrated by the significant bonding contribution to the s−d component of the Pt−Pt bond Hamilton population toward the bottom of the d band. This interaction is also partially responsible for the bonding contributions to the Pt(s)−Pt(s) component of the Pt−Pt bond Hamilton population in the vicinity of the bottom of the d band, the remainder of the s−s interaction being derived from states that are principally Pt(s) in character.

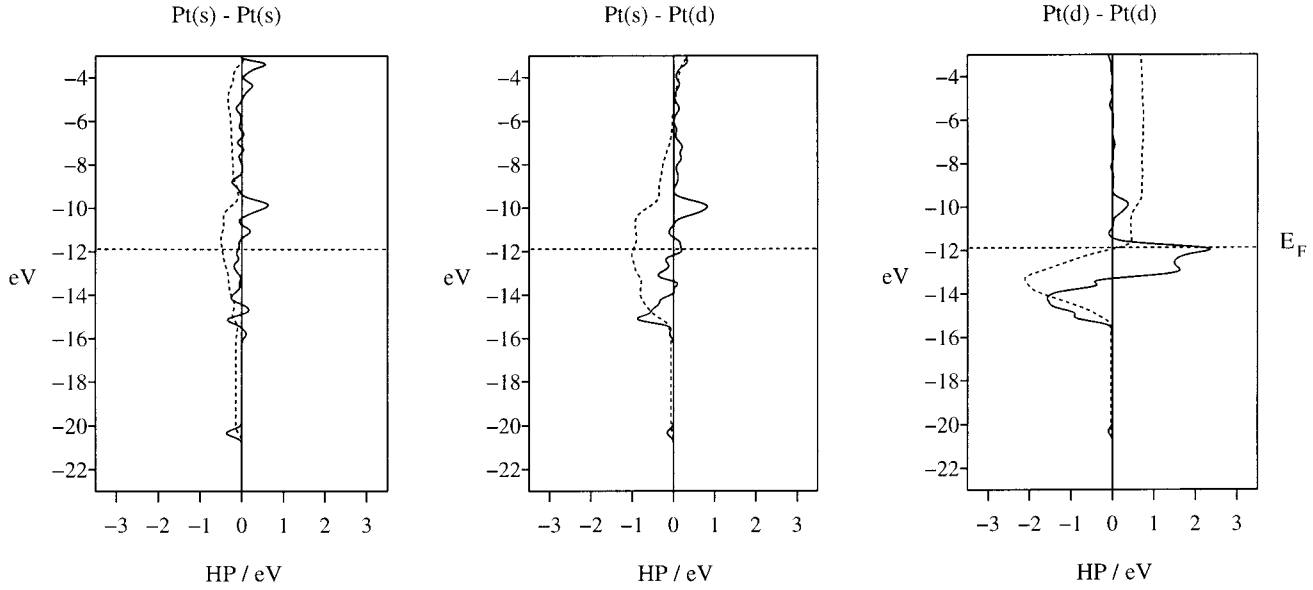

Figure 11. Energy resolved s−s, s−d, and d−d components of the Pt−Pt surface bond directly below a bridging CO molecule for the p(2 × 2)-CO/Pt(111) chemisorption system. The numerical value of each component is given by the intersection of the integration (vertical dashed line) and the Fermi level, ϵ_F.

TABLE 17: Summary of the s−s, s−d, and d−d Components of the Pt−Pt Bond Hamilton Population for a Clean Pt(111) Surface and for the Pt−Pt Bond Directly below a Bridging CO

	C−O bond HP/eV		
Pt−Pt bond	Pt(s)−Pt(s)	Pt(s)−Pt(d)	Pt(d)−Pt(d)
clean Pt(111) surface	−0.79	−1.56	0.23
under bridging CO	−0.68	−1.37	0.01

In Figure 11 the s−s, s−d, and d−d components of the Pt−Pt bond Hamilton population for the Pt−Pt surface bond directly below chemisorbed CO on the bridging site are shown for comparison. The s−s, s−d, and d−d components of the Pt−Pt bond Hamilton populations shown in Figures 10 and 11 are summarized in Table 17.

The d−d component of the Pt−Pt bond Hamilton population in Figure 11 appears relatively unchanged from that on the clean Pt(111) surface (Figure 10). However, the s−d component of the interaction is significantly reduced due to the reduction in the number of Pt(s) states available for Pt−Pt bonding on chemisorbing CO. The reduced Pt(s) DOS clearly manifests itself in the sizable reductions in the s−s component of the Pt−Pt bond Hamilton population in the region just above the Fermi level. We have also observed an analogous reduction in the p−d component of the Pt−Pt bond Hamilton population. Thus CO chemisorption is responsible for significant reductions in both the s−d and p−d components of the Pt−Pt bond Hamilton population, the only major contributions to Pt−Pt bonding aside from the d−d interaction.

Our experiences with the Pt, Cu, and Al(111) surfaces suggest that the changes in bonding within the surface layer that accompany chemisorption are essentially localized in those surface bonds that involve atoms directly bonded to chemisorbed CO. The 2- and 3-fold bridge and hollow sites (see Figure 2) afford better overlap between the surface bands and the CO bands, thus we might anticipate a greater reduction in the numbers of surface s and p states available for bonding within the surface for the higher coordination sites. This is indeed the case for all three surfaces.

Tables 18 and 19 summarize the changes in surface−CO, C−O, and surface bonding that accompany CO chemisorption

TABLE 18: Bond Hamilton Population Analysis for CO Chemisorption on the Top, Bridge, and Hollow Sites of the Pt(111) Surface

Pt(111) site	Δ*HP*(Pt−CO)/eV	Δ*HP*(Pt−Pt)/eV	Δ*HP*(C−O)/eV
top	−18.43	0.24	0.64
bridge	−23.46	2.13	3.90
fcc hollow	−22.53	2.18	4.57
hcp hollow	−24.12	2.37	5.17

TABLE 19: Bond Hamilton Population Analysis for CO Chemisorption on the Top, Bridge, and Hollow Sites of the Cu(111) Surface

Cu(111) site	Δ*HP*(Cu−CO)/eV	Δ*HP*(Cu−Cu)/eV	Δ*HP*(C−O)/eV
top	−16.34	4.58	6.25
bridge	−25.92	9.46	11.58
fcc hollow	−27.22	10.69	13.44
hcp hollow	−27.25	10.62	13.38

on the top, bridge, and hollow sites of the Pt(111) and Cu(111) surfaces. The changes in the bond Hamilton populations are calculated with respect to those for a clean surface and a p(2 × 2) array of CO molecules. The slab geometries for the clean and CO-covered surfaces are identical, i.e., the atom positions within the slab are fixed while the CO layer is relaxed on the surface. This allows us to focus our attention on the change in metal−metal bonding that results from the interaction between CO and the surface states. Co-relaxation of the CO layer and the top two layers of the slab results in modest variations in the positions of the metal atoms relative to the fixed slab calculation. In the case of top and bridge site chemisorption on the Pt(111) surface, these variations result in changes of between 1% and 2% in the surface−CO, C−O, and metal−metal bond Hamilton populations. Thus we ascribe an uncertainty of ± 2% to each of the Hamilton populations reported in Table 18. Further, we ascribe a 2% uncertainty to the corresponding Hamilton populations reported in Tables 19 and 20 for the CO/Cu(111) and CO/Al(111) chemisorption systems. This level of uncertainty is not sufficient to alter any of the conclusions reached on the basis of our analysis.

We note the basic feature of productive chemisorption: increased metal−adsorbate bonding at the expense of bonding within both the surface and the adsorbate.[32] From Tables 18

TABLE 20: Bond Hamilton Population Analysis for CO Chemisorption on the Top, Bridge, and Hollow Sites of the Al(111) Surface

Al(111) site	ΔHP(Al−CO)/eV	ΔHP(Al−Al)/eV	ΔHP(C−O)/eV
top	−2.19	−10.47	24.74
bridge	−9.99	−0.58	22.27
fcc hollow	−11.49	0.11	22.00
hcp hollow	−13.17	1.96	21.75

and 19 we note both the anticipated increase in the surface−CO bond Hamilton population for the higher coordinate chemisorption sites and the corresponding decrease in the surface bond Hamilton population resulting from the reduced availability of surface s and p bands for bonding within the surface layer. The increased reduction in C−O bonding for CO chemisorbed on the higher coordinate sites can be correlated directly with the increased occupancy of the CO(2π) band (see Table 9) for CO chemisorption on the higher coordinate sites of the Pt and Cu(111) surfaces.

Interestingly, if we combine the changes in the surface−CO, C−O, and surface bonding summarized in Tables 18 and 19, we end up with a change in the total bond Hamilton population that favors top site chemisorption on both the Pt(111) and Cu(111) surfaces. Although it is encouraging that we might be able to construct a measure of structural stability for these systems on the basis of the change in the total bond Hamilton population, we choose to remember that our extended Hückel treatment of the problem is, in essence, a qualitative treatment of orbital interactions.

Indeed, we note that despite our success in predicting the experimentally determined chemisorption site preferences for CO chemisorbed on the Pt and Cu(111) surfaces, we are unable to reproduce the preference for top site chemisorption on the Al(111) surface. The changes in the surface−CO, C−O, and surface bond Hamilton populations for CO chemisorbed on the top, bridge, and hollow sites of the Al(111) surface are summarized in Table 20, and when combined result in a preference for CO chemisorption on the higher coordinate sites.

From Tables 18, 19, and 20 we note that in order to calculate the energetically preferred chemisorption site for CO, it is necessary, for all three surfaces, to consider a relatively modest variation in the total bond Hamilton population resulting from significantly larger variations in the surface−CO, C−O, and surface bond Hamilton populations. Thus we are not surprised that our essentially qualitative treatment of orbital energetics fails to consistently reproduce the rather subtle preference for top site chemisorption on the Pt, Cu, and Al(111) surfaces. In situations such as this, our purpose is best served by focusing our attention on the site dependence of the individual bond Hamilton populations contributing to the variation in the total bond Hamilton population.

From Table 20 we note that, for CO chemisorbed on the Al(111) surface, increased surface−CO orbital overlap results in an increased surface−CO bond Hamilton population for the higher coordinate sites. As noted previously for CO chemisorption on the Pt and Cu(111) surfaces, CO chemisorption on the higher coordinate sites of the Al(111) surface results in less s and p surface states available for bonding within the surface layer and a correspondingly lower surface bond Hamilton population.

We also note that for CO chemisorbed on the Al(111) surface, the decrease in the occupation of the CO(2π) band for CO chemisorbed in the higher coordination sites contrasts the increased CO(2π) band occupancy for CO chemisorbed on the higher coordinate sites of both the Pt and Cu(111) surfaces (see Table 9). This difference is reflected in the site dependent variation in the C−O bond Hamilton population given in Table 20.

XII. Conclusion

We have noted significant differences between the traditional, frontier orbital description of surface−CO bonding offered by Blyholder's model and our descriptions of surface−CO bonding based on the Hamilton population formalism. In addition to the interactions between the frontier orbitals on CO and the surface d band, we have found it necessary to incorporate both the low-lying CO(4σ) orbital and the surface s and p bands into our model for CO chemisorption on the Pt(111) and Cu(111) surfaces.

For CO chemisorbed on both the Pt(111) and Cu(111) surfaces, in excess of 95% of the surface−CO interaction can be attributed to interactions involving the CO 4σ, 5σ, and 2π orbitals. This three-orbital basis on CO is also capable of reproducing the chemisorption site-dependent variation in surface−CO bonding on the Al(111) surface.

Our Hamilton population description of surface−CO bonding highlights the dominant contributions made by the surface s and p bands. With the exception of the π component of surface−CO bonding on the Pt(111) surface, the surface s and p bands dominate the interactions between CO and the Pt, Cu, and Al(111) surfaces.

The Pt d band dominated π component of surface−CO bonding in the CO/Pt(111) chemisorption system reminds us that the platinum and copper surfaces have somewhat different properties. The sizable interaction between the low-lying Al(s) band and the CO 3σ, 4σ, and 1π bands indicates the still greater differences in the properties of the Al(111) surface.

We believe that the models of both the σ and π components of surface−CO bonding resulting from our analysis can be applied, with little or no modification, to the study of surface−adsorbate interactions involving adsorbates with either the σ-donor or π-acceptor characteristics of CO.

Acknowledgment. We are grateful to the National Science Foundation for its support of this work by Research Grant CHE 99-70089.

References and Notes

(1) Glassey, W. V.; Papoian, G. A.; Hoffmann, R *J. Chem. Phys.* **1999**, *111*, 893.
(2) Bockstedte, M.; Kley, A.; Neugebauer. J.; Scheffler, M. *Comput. Phys. Comm.* **1997**, *107*, 187.
(3) Troullier, N.; Martins, J. L. *Phys. Rev. B* **1991**, *43*, 1993.
(4) Kleinman, L.; Bylander, D. M. *Phys. Rev. Lett.* **1982**, *48*, 1425.
(5) Gonze, X.; Stumpf, R.; Scheffler, M. *Phys. Rev. B* **1991**, *44*, 8503.
(6) Monkhorst, H. J.; Pack, J. D. *Phys. Rev. B* **1976**, *13*, 5188.
(7) Perdew, J. P.; Zunger, A. *Phys. Rev. B* **1981**, *23*, 5048.
(8) *CRC Handbook of Chemistry and Physics*, 80th ed.; CRC Press: Boca Raton, FL, 1999.
(9) Aizawa, H.; Tsuneyuki, S. *Surf. Sci.* **1998**, *399*, L364.
(10) Philipsen, P. H. T.; te Velde, G.; Baerends, E. J. *Chem. Phys. Lett.* **1994**, *226*, 583.
(11) Müller, J. E. *Surf. Sci.* **1986**, *178*, 589.
(12) See ref 11 and references contained therein.
(13) Persson, B. N. J.; Müller, J. E. *Surf. Sci.* **1986**, *171*, 219.
(14) Perdew, J. P.; Wang, Y. *Phys. Rev. B* **1992**, *45*, 13244.
(15) Pritchard, J. *Surf. Sci.* **1979**, *79*, 231.
(16) Hollins, P.; Pritchard, J. *Surf. Sci.* **1979**, *89*, 486.
(17) Jugnet, Y.; Duc, T. M. *Chem. Phys. Lett.* **1978**, *58*, 243.
(18) Steininger, H.; Lehwald, S.; Ibach, H. *Surf. Sci.* **1982**, *123*, 264.
(19) Flodström, S. A.; Martinsson, C. W. B. *Appl. Surf. Sci.* **1982**, *10*, 115.
(20) Paul, J.; Hoffmann, F. M. *Chem. Phys. Lett.* **1986**, *130*, 160.
(21) Khonde, K.; Darville, J.; Gilles, J. M. *Surf. Sci.* **1983**, *126*, 414.

(22) Hu, P.; King, D. A.; Lee, M.-H.; Payne, M. C. *Chem. Phys. Lett.* **1995**, *246*, 73.
(23) Landrum, G. A.; Glassey, W. V. *bind v3.0*, 1999. Bind is available as part of the YAeHMOP extended Hückel package on the WWW at URL: http://overlap.chem.cornell.edu:8080/
(24) Landrum, G. A. *viewkel v3.0*, 1999. Viewkel is available as part of the YAeHMOP extended Hückel package on the WWW at URL: http://overlap.chem.cornell.edu:8080/
(25) Blyholder, G. J. *J. Phys. Chem.* **1964**, *68*, 2772.
(26) Wong, Y.-T.; Hoffmann, R. *J. Phys. Chem.* **1991**, *95*, 859.
(27) Bagus, P. S.; Pacchioni, G. *Surf. Sci.* **1992**, *278*, 427.
(28) Hammer, B.; Morikawa, Y.; Norskov, J. K. *Phys. Rev. Lett.* **1996**, *76*(12), 2141.
(29) Ishi, S.; Ohno, Y.; Viswanathan, B. *Surf. Sci.* **1985**, *161*, 349.
(30) Doyen, G.; Ertl, G. *Surf. Sci.* **1977**, *69*, 157.
(31) Glassey, W. V.; Bowen, S. Work in progress.
(32) Hoffmann, R. *Solids and Surfaces: A Chemist's View of Bonding in Extended Structures*; VCH: New York, 1988; p75−76.